

ratio would be 1, suggesting that the hadronic neutral current has a parity-nonconserving interference term and that a purely vector form is unlikely. Larger ν and $\bar{\nu}$ exposures are currently being analyzed to provide a more quantitative test of the gauge models which involve the neutral currents.⁹

We thank the staff of the Brookhaven National Laboratory for their strong support during this work. J. Blandino and J. McElaney of the Harvard University High Energy Physics Laboratory were responsible for the mechanics of the drift chambers and calorimeters; L. Holcomb and H. Weedon implemented the electronic data acquisition systems for the chambers and calorimeter.

*Work supported in part by the U. S. Energy Research and Development Administration.

¹L. Sulak *et al.*, unpublished; H. H. Williams *et al.*, in Proceedings of the International Conference on the Production of Particles with New Quantum Numbers, Madison, Wisconsin, May 1976 (to be published); D. Cline *et al.*, Phys. Rev. Lett., **37**, 252 (1976).

²B. Escoubes *et al.*, Colloq. Int. CNRS **245**, 265 (1975).

³L. Sulak, in *Proceedings of Calorimeter Workshop*, edited by M. Atac (Fermi National Accelerator Laboratory, Batavia, Ill., 1975), p. 155.

⁴D. C. Cheng *et al.*, Nucl. Instrum. Methods **117**, 157

(1974).

⁵The neutrino and antineutrino spectra have been calculated by T. Tso at Brookhaven National Laboratory using the Stanford-Wang parametrization of π and K spectra [BNL Reports No. BNL 11299 JRS/CLW-1 and No. JRS/CLW-2 (unpublished)].

⁶The energy spectrum of neutrons is obtained from the total energy deposited by multicluster, in-time events. It falls as $\exp(-T/100 \text{ MeV})$. The $np \rightarrow np$ cross sections $d\sigma/du$ are taken from a compilation by M. Roos *et al.*, UCRL Report No. UCRL 20000 NN, August 1970 (unpublished).

⁷M. Rollier *et al.*, Colloq. Int. CNRS **245**, 349 (1975). From the q^2 distribution for $\bar{\nu}p \rightarrow \mu^+n$ occurring in Freon, m_A was measured to be $0.91 \pm 0.12 \text{ GeV}/c^2$.

⁸Events from the reaction $\nu n \rightarrow \nu$ would appear in our sample if np charge exchange occurs in the target nucleus or if it occurs after the neutron leaves the nucleus, provided that the de-excitation of target goes undetected i.e., less than 3 MeV of energy is deposited in the scintillator). We are currently evaluating the probability of these processes.

⁹S. Weinberg, Phys. Rev. D **5**, 1412 (1972); J. J. Sakurai and L. F. Urrutia, Phys. Rev. D **11**, 159 (1975); A. De Rújula, H. Georgi, and S. L. Glashow, Phys. Rev. D **12**, 3589 (1975); J. T. Gruenwald *et al.*, Bull. Am. Phys. Soc. **21**, 17 (1976); H. Fritzsch, M. Gell-Mann, and P. Minkowski, Phys. Lett. **59B**, 256 (1975); F. Wilczek, A. Zee, R. L. Kingsley, and S. B. Treiman, Phys. Rev. D **12**, 2768 (1975); M. Barnett, Phys. Rev. Lett. **34**, 41 (1975), and Phys. Rev. D **11**, 3246 (1975); S. Pakvasa, W. A. Simmons, and S. F. Tuan, Phys. Rev. Lett. **35**, 703 (1975).

Inclusive Pion Electroproduction at Large p_T [†]

A. Browman,* K. M. Hanson,* S. D. Holmes, R. V. Kline, D. Larson, F. M. Pipkin, S. W. Raither, and A. Silverman

Laboratory for Nuclear Studies, Cornell University, Ithaca, New York 14853, and High Energy Physics Laboratory, Harvard University, Cambridge, Massachusetts 02138

(Received 9 February 1976)

We report measurements of the inclusive electroproduction reaction $ep \rightarrow e\pi^+X$ for pions produced at 90° in the virtual-photon-proton center-of-mass system. Data are presented at the (W, Q^2) points $(2.2 \text{ GeV}, 1.2 \text{ GeV}^2)$, $(2.2, 3.6)$, $(2.65, 1.2)$, $(2.65, 2.0)$, $(2.65, 2.8)$, $(2.65, 3.6)$, $(3.1, 1.2)$, and $(3.1, 2.0)$. The invariant structure function is studied as a function of W , Q^2 , x_T , p_T^2 , and the square of the invariant undetected mass.

There has been great interest recently in investigating hadronic processes in which a particle is produced with a large transverse momentum. It is believed that the short-distance structure of the hadrons is reflected in the behavior of such processes.¹ In experiments carried out at the CERN intersecting storage rings² and Fermi National Accelerator Laboratory,³ it has been found that pions produced in p - p collisions at 90° in the

center-of-mass system suggest a simple scaling law,

$$E d^3\sigma/dp^3 = f(x_T)/W_n, \quad n \sim 8 \text{ to } 11. \quad (1)$$

Here W is the total energy of the virtual-photon, target-proton system and $x_T = p_T/p_{\text{max}}^*$, where p_T is the momentum of the pion transverse to the virtual-photon direction and p_{max}^* is the maximum kinematically allowed momentum of the pion

in the virtual-photon-proton center-of-mass system. The magnitude of the exponent n is difficult to understand in terms of the wide-angle scattering of pointlike constituents of the colliding hadrons^{4,5} but it can be understood in the framework of the constituent interchange model.^{1,6-8}

We report here measurements carried out at the Wilson Synchrotron Laboratory on the electroproduction reaction

$$e + p \rightarrow e + \pi^+ + \text{anything} \quad (2)$$

which is viewed as the virtual-photoproduction reaction

$$\gamma_v + p \rightarrow \pi^+ + \text{anything}. \quad (3)$$

The square of the virtual-photon mass $-Q^2$, the energy ν , and the direction and polarization parameter ϵ are tagged by the detected electron. The cross section for Reaction (2) is written

$$d\sigma/d\Omega_e dE_e dp_{\pi^3} = \Gamma d^3\sigma/dp_{\pi^3}, \quad (4)$$

where Γ is the "flux" of virtual photons.⁹ $d^3\sigma/dp_{\pi^3}$ is the cross section for Reaction (3) and is a function of W , Q^2 , ϵ , x_T (or p_T), and x (or M_x^2 , the square of the invariant undetected mass). Here $x = p_L^*/p_{\text{max}}^*$, where p_L^* is the component of the pion momentum along the virtual-photon direction and the asterisk denotes the virtual-photon-proton center-of-mass system. For all the data reported here $-0.05 < x < 0.05$ and $0.8 < \epsilon < 0.95$.

The data are presented in terms of the invariant structure function,

$$F = \frac{E}{\sigma_T} \frac{d^3\sigma}{dp^3} = \frac{2W}{\sigma_T p^*} \frac{d\sigma}{d\Omega_{\pi^*} dM_x^2}. \quad (5)$$

Here σ_T is the total virtual-photon-proton cross section for the W , Q^2 , and ϵ of the reaction. σ_T was taken from a fit to the Stanford Linear Accelerator Laboratory-Massachusetts Institute of Technology measurements of νW_2 with the assumption that the ratio of the scalar to transverse component was 0.18.¹⁰

A two-arm spectrometer system was used to obtain data at the (W, Q^2) points (2.2 GeV, 1.2 GeV²), (2.2, 3.6), (2.65, 1.2), (2.65, 2.0), (2.65, 2.8), (2.65, 3.6), (3.1, 1.2), and (3.1, 2.0). A more complete description of the apparatus is given by Browman *et al.*¹¹ A lead-Lucite shower counter served to identify the scattered electrons. Pions were identified by a threshold gas Cherenkov counter when their momenta were greater than 1.5 GeV/ c and by time of flight at lower momenta. The data have been corrected for random coinci-

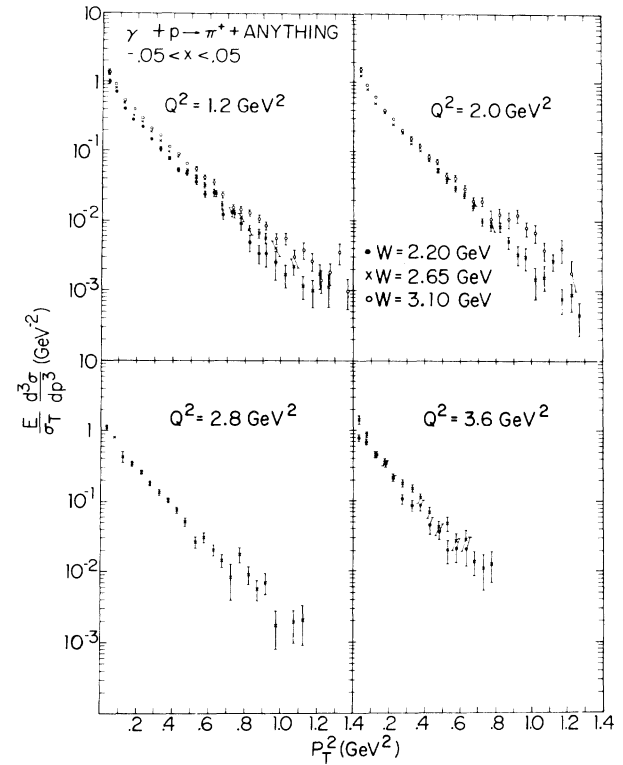


FIG. 1. The p_T^2 dependence of the π^+ invariant structure function for the eight (W, Q^2) points.

dences ($\sim 1\%$), electronics dead time ($\sim 7\%$), target-wall background ($\sim 5\%$), absorption in the counters ($\sim 5\%$), pion decay losses ($\sim 3\%$), and electron misidentification ($\sim 5\%$). The uncertainties shown are statistical only and do not include possible systematic errors estimated to be less than $\pm 8\%$. The data have not been corrected for radiative processes. Calculations indicate that the radiative correction is less than 15% for $x_T < 0.75$ for all W and Q^2 , and on a 10% level is independent of W and Q^2 in the region $x_T > 0.75$.

Figure 1 shows a plot of the invariant structure function versus p_T^2 for the eight (W, Q^2) points. The data indicate a change in slope at $p_T^2 = 0.15$ GeV². We have fitted the data by the form $a \times \exp(-bp_T^2)$ in the regions $p_T^2 < 0.15$ GeV² and $p_T^2 > 0.15$ GeV². The results of the fits are given in Table I. There appears to be a systematic decrease of b with increasing W and no dependence of b on Q^2 for $p_T^2 > 0.15$ GeV², while in the region $p_T^2 < 0.15$ GeV², b is independent of both W and Q^2 within statistical variations. The results presented here are consistent with results of the inclusive π^- electroproduction experiment carried out at DESY.¹² In the region $-0.2 < x < 0.2$, $p_T^2 < 0.4$ GeV², $0.5 \text{ GeV}^2 < Q^2 < 1.5 \text{ GeV}^2$, they find the slope

TABLE I. Fits of the invariant structure function by the form $a \exp(-bp_T^2)$ for the regions $p_T^2 < 0.15 \text{ GeV}^2$ and $p_T^2 > 0.15 \text{ GeV}^2$. b is given in units of GeV^{-2} .

W (GeV)	Q^2 (GeV^2)	$b(p_T^2 < 0.15)$	$b(p_T^2 > 0.15)$
2.2	1.2	10.4 ± 0.6	6.1 ± 0.1
2.65	1.2	10.3 ± 0.5	5.9 ± 0.1
3.1	1.2	10.3 ± 0.6	5.4 ± 0.1
2.65	2.0	9.4 ± 0.4	6.1 ± 0.1
3.1	2.0	10.5 ± 0.8	5.6 ± 0.2
2.65	2.8	9.4 ± 0.7	6.2 ± 0.2
2.2	3.6	7.0 ± 1.2	7.7 ± 0.6
2.65	3.6	11.5 ± 1.0	6.0 ± 0.3

to be $b = 9.0 \pm 1.1 \text{ GeV}^2$ at $W = 2.0 \text{ GeV}$ and $b = 8.1 \pm 0.7 \text{ GeV}^2$ at $W = 2.5 \text{ GeV}$. Analogous photoproduction data have been reported by Moffeit *et al.*,¹³ Burfeindt *et al.*,¹⁴ Kaune *et al.*,¹⁵ and Boyarski *et al.*¹⁶

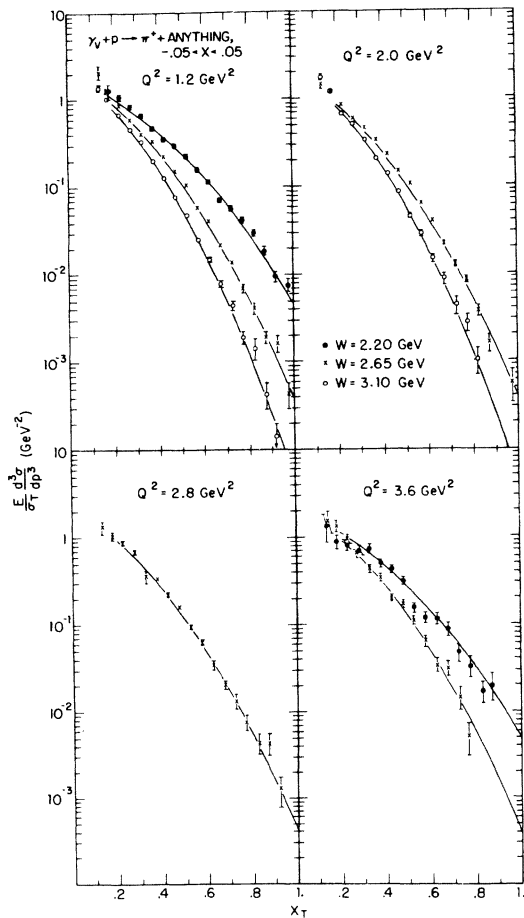


FIG. 2. Plots of the invariant structure function versus the scaling variable x_T for the eight (W, Q^2) points. At each energy the curves shown are independent of Q^2 .

Figure 2 shows the structure function for π^+ versus x_T for the eight (W, Q^2) points. The data show that the structure function is independent of Q^2 , a feature¹⁷ which has also been observed for $x > 0.1$ and $p_T^2 < 0.02 \text{ GeV}^2$. However, the W dependence is much different from the one for the forward data. In the forward direction the structure function at fixed x is a weak function of W .¹⁷ The data at $x = 0$ show that the structure function has a strong W dependence for x_T larger than 0.2. Assuming that the structure function is given by the form

$$F = f(x_T)/W^n, \tag{6}$$

we have found the W dependence at fixed x_T to be described by the expression

$$n(x_T) = (13.41 \pm 0.38)x_T^{1.71 \pm 0.05}. \tag{7}$$

Figure 3 shows a plot of n versus x_T . The dependence of n on x_T means that the data do not scale in the sense of Eq. (1). We have also determined that the data cannot be represented by the alternative form

$$F(x_T, p_T) = f(x_T)g(p_T), \tag{8}$$

which includes, as a special case,

$$F(x_T, p_T) = f(x_T)/(p_T^2 + M^2)^n. \tag{9}$$

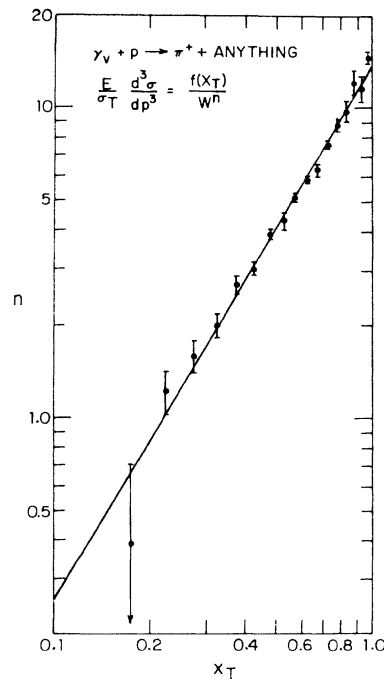


FIG. 3. A plot of the fit parameter n versus x_T for π^+ production.

The solid curves in Fig. 2 are a fit by the form

$$F = [\exp P(x_T)] / W^{n(x_T)} (Q^2)^m, \quad (10)$$

where $n(x_T)$ is given above and $P(x_T)$ is a cubic polynomial. The fit gives for the Q^2 dependence $m = -0.02 \pm 0.02$. This gives a quantitative measure of the independence of Q^2 .

An alternate way to view the inclusive cross section is in terms of the missing mass and the minimal exclusive cross sections to which the inclusive cross section is linked in the correspondence-principle limit.¹⁸ At a fixed missing mass, the constituent interchange model suggests that the cross section should have the form^{1,7,8}

$$d\sigma/d\Omega_n^* dM_X^2 = \sum_i P_i(M_X^2) / W^{2n_i-6}, \quad (11)$$

where n_i is equal to the number of elementary fields in the i th exclusive limit channel and P is a polynomial in the square of the missing mass. For inclusive π^+ production two connecting exclusive channels are

$$\gamma_v + p \rightarrow \pi^+ + n, \quad (12)$$

$$\gamma_v + p \rightarrow \pi^+ + \pi^- + p. \quad (13)$$

For the first reaction $n_i = 9$; for the second $n_i = 11$. In the constituent interchange model each of these reactions is linked to a number of quark reactions allowed by the exchange or interchange of quark fields using the elementary two-field meson and three-field baryon wave functions. For Reaction (12) three such reactions are⁷

$$\gamma + q \rightarrow M + q, \quad (14)$$

$$\bar{q} + B \rightarrow M + qq, \quad (15)$$

$$\gamma + B \rightarrow M + B^*. \quad (16)$$

Each of these reactions has a different dependence on the missing mass.

Figure 4 shows the inclusive pion cross section as a function of W and square of the missing mass for $Q^2 = 1.2 \text{ GeV}^2$. The solid curves are a fit by the expression

$$d\sigma/d\Omega_n^* dM_X^2 = P(M_X^2) / W^n, \quad (17)$$

where $P(M_X^2)$ is a cubic polynomial in M_X^2 . The best-fit value is $n = 12.69 \pm 0.13$, independent of M_X^2 .

The exclusive reaction $\gamma_v + p \rightarrow \pi^+ + n$ has been found to have a W dependence,¹¹

$$d\sigma/d\Omega_n^* \approx 1/W^{12.65 \pm 0.40}. \quad (18)$$

The quark counting rules predict that the exclusive reaction should have a $1/W^{12}$ dependence.¹⁹

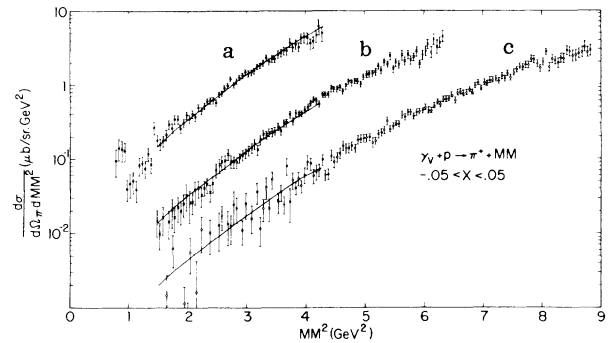


FIG. 4. $d\sigma/d\Omega_n^* dM_X^2$ as a function of the square of the missing mass for $Q^2 = 1.2 \text{ GeV}^2$ and three values of W : curve a, $W = 220 \text{ GeV}$; curve b, 2.65 GeV ; curve c, 310 GeV . The solid curves are fits by the form $d\sigma/d\Omega_n^* \times dM_X^2 = P(M_X^2) / W^n$, where $P(M_X^2)$ is a cubic polynomial.

The agreement among the values of n derived from the measurements of the inclusive cross section, the limiting exclusive cross section, and the prediction of the quark counting rules gives strong support to the constituent interchange model.

In conclusion, the data show that the invariant structure function is independent of Q^2 and, in this energy range, does not display the simple scaling behavior observed in purely hadronic reactions. However, it must be kept in mind that the measurements reported here are at a much lower value of p_T than those of Refs. 2 and 3. When expressed in terms of the square of the missing mass, the inclusive cross section displays a dependence on the center-of-mass energy W which is independent of the square of the missing mass and is the same as that found for the inclusive reaction $\gamma_v + p \rightarrow \pi^+ + n$. This latter behavior supports the predictions of the constituent interchange model and the correspondence principle, indicating that in this energy region the cross section is dominated by elementary quark interactions of the form given by Eqs. (14)–(16). The failure to observe scaling in the form predicted by Eq. (1) may be due to the fact that no single one of the elementary quark interactions dominates in this energy region.

We wish to acknowledge the support of Professor Boyce McDaniel, the staff of the Wilson Synchrotron Laboratory, and the staff of the Harvard University High Energy Physics Laboratory.

†Research supported in part by the U. S. Energy Research and Development Administration (Harvard) and

in part by the National Science Foundation (Cornell).

*Present address: Clinton P. Anderson Laboratory, Los Alamos, New Mex. 87545.

¹For a recent review see D. Sivers, S. J. Brodsky, and R. Blankenbecler, Phys. Rep. 23C, 1 (1976).

²F. W. Busser *et al.*, Phys. Lett. 46B, 471 (1973).

³J. W. Cronin *et al.*, Phys. Rev. D 11, 3105 (1975).

⁴S. M. Berman, J. D. Bjorken, and J. B. Kogut, Phys. Rev. D 4, 3388 (1971).

⁵For a somewhat different interpretation see R. C. Hwa, A. J. Spiessbach, and M. J. Teper, Phys. Rev. Lett. 36, 1418 (1976).

⁶R. Blankenbecler, S. J. Brodsky, and J. F. Gunion, Phys. Lett. 42, (1972), and Phys. Rev. D 6, 2652 (1972).

⁷R. Blankenbecler and S. J. Brodsky, Phys. Rev. D 10, 2973 (1974).

⁸R. Blankenbecler, S. J. Brodsky, and J. Gunion,

Phys. Rev. D 12, 3469 (1975).

⁹L. N. Hand, Phys. Rev. 129, 1834 (1964).

¹⁰W. B. Atwood, private communication.

¹¹A. Browman *et al.*, Phys. Rev. Lett. 35, 1313 (1975).

¹²V. Eckardt *et al.*, DESY Report No. 74/5, 1974 (unpublished).

¹³K. C. Moffeit *et al.*, Phys. Rev. D 5, 1603 (1972).

¹⁴H. Burfeindt *et al.*, Phys. Lett 43B, 345 (1973), and Nucl. Phys. B74, 189 (1974).

¹⁵W. Kaune *et al.*, Phys. Rev. D 11, 478 (1975).

¹⁶A. M. Boyarski *et al.*, SLAC Report No. SLAC-PUB-1694, 1975 (unpublished).

¹⁷C. J. Bebek *et al.*, Phys. Rev. Lett. 34, 759 (1975).

¹⁸J. D. Bjorken and J. Kogut, Phys. Rev. D 8, 1341 (1973).

¹⁹S. J. Brodsky and G. R. Farrar, Phys. Rev. Lett. 31, 1153 (1973).

Electromagnetic Mass Differences and Decay Rates of Charmed Mesons in the Charmed-Quark Model

Seiji Ono*

III Physikalisches Institut, Technische Hochschule Aachen, Aachen, West-Germany

(Received 1 July 1976)

Using the harmonic-oscillator charmed-quark model, I have studied the electromagnetic mass differences and the decay rates of charmed mesons.

A new particle D^0 with a mass of 1.86 GeV has recently been discovered.¹ This particle has properties of a charmed meson.^{1,2} In this note I study the properties of charmed mesons using the charmed-quark model. In a previous paper³ the electromagnetic mass differences of baryons, the amplitudes for the processes $\gamma N \rightarrow N^* \rightarrow N\pi$, and the cross sections for the processes $eN \rightarrow eN^*$ were explained with remarkable success using explicit harmonic-oscillator wave functions with a radius $R^2 = 2.75 \text{ GeV}^{-2}$ consistently. In an analogous way I studied the electromagnetic properties of mesons⁴ and found almost the same radius $R^2 = 2.74 \text{ GeV}^{-2}$ for the $q\bar{q}$ wave function.

Following Refs. 3 and 4 I make the following assumptions on the charmed mesons: (a) The electromagnetic mass differences of charmed mesons are caused (i) by the mass difference (Δm_e) between the u quark and the d quark, (ii) by the Coulomb force between the quark and the antiquark, and (iii) by the magnetic hyperfine interaction. (b) The gyromagnetic ratios of quarks are 1. Therefore, the magnetic moment equals charge/ $2 \times$ mass. From the magnetic moments of baryons we get $\mu_q = \mu_p = 2.793e/2m_p$, hence $m_q \sim 336 \text{ MeV}$ for the u quark and for the d quark. (c) From the mass spectrum of mesons (ψ, D^0, ρ, π , etc.),

I estimate the mass of the charmed quark (m_c) to be about 1300 MeV.

Employing the harmonic-oscillator wave function for the $c\bar{q}$ system,

$$\psi = N \exp(-r^2/2R_0^2), \quad R_0 = \sqrt{2}R, \quad (1)$$

one gets

$$\begin{aligned} D^+ - D^0 &= -\Delta m_e + \frac{2}{3} \left(\frac{2}{\pi} \right)^{1/2} \frac{e^2}{R} \\ &\quad + \frac{2}{3} \left(\frac{2}{\pi} \right)^{3/2} R^{-3} \pi \mu_p^2 \frac{m_q}{m_c}, \\ D^{*+} - D^{*0} &= -\Delta m_e + \frac{2}{3} \left(\frac{2}{\pi} \right)^{1/2} \frac{e^2}{R} \\ &\quad - \frac{2}{9} \left(\frac{2}{\pi} \right)^{3/2} R^{-3} \pi \mu_p^2 \frac{m_q}{m_c}. \end{aligned} \quad (2)$$

Here D and D^* denote, respectively, the charmed pseudoscalar and vector mesons of isospin $\frac{1}{2}$.

At present we have no experimental data to determine the value of R directly. In previous papers^{3,4} from electromagnetic properties of baryons and mesons I obtained

$$R_{qq} \approx R_{q\bar{q}} \approx 2R_{c\bar{c}}, \quad R_{q\bar{q}}^2 \approx 2.74 \text{ GeV}^{-2}. \quad (3)$$

Therefore, it seems most reasonable (see sec-